INVITED PAPER *Special Section on Recent Advances in Photonics Technologies and Their Applications*

Integrated Photonic Devices and Applications for 100GbE-and-Beyond Datacom

Yoshiyuki DOI[†a)], **Takaharu OHYAMA**[†], **Toshihide YOSHIMATSU**[†], **Tetsuichiro OHNO**[†], **Yasuhiko NAKANISHI**[†], **Shunichi SOMA**[†], **Hiroshi YAMAZAKI**[††], **Manabu OGUMA**[††], **Toshikazu HASHIMOTO**[††], ***and*** **Hiroaki SANJOH**[†], ***Members***

SUMMARY We review recent progress in integrated photonics devices and their applications for datacom. In addition to current technology used in 100-Gigabit Ethernet (100GbE) with a compact form-factor of the transceiver, the next generation of technology for 400GbE seeks a larger number of wavelengths with a more sophisticated modulation format and higher bit rate per wavelength. For wavelength scalability and functionality, planar lightwave circuits (PLCs), such as arrayed waveguide gratings (AWGs), will be important, as well higher-order-modulation to ramp up the total bit rate per wavelength. We introduce integration technology for a 100GbE optical sub-assembly that has a 4λ x 25-Gb/s non-return-to-zero (NRZ) modulation format. For beyond 100GbE, we also discuss applications of 100GbE sub-assemblies that provide 400-Gb/s throughput with 16λ x 25-Gb/s NRZ and bidirectional 8λ x 50-Gb/s four-level pulse amplitude modulation (PAM4) using PLC cyclic AWGs.

key words: *integrated photonics, datacom, 100GbE/400GbE, optical sub-assembly, arrayed waveguide grating*

1. Introduction

Recent innovations such as big data, cloud computing, and the Internet of Things (IoT) are driving the expansion of datacom networks in datacenters and mobile backhaul with a rapid growth rate of over 20% annually [1]. In order to meet the bit rate requirements in a timely manner, the IEEE 100-Gb/s Ethernet (100GbE) for datacom links has already been commercialized [2]. Furthermore, the next generation, 400-Gb/s Ethernet (400GbE), is being discussed for standardization [3] with regards to technical feasibility and cost-effectiveness.

Figure 1 shows recent research trends in 100GbE-and-beyond datacom. For 100-Gb/s throughput, 10-km 100GbE (100GBASE-LR4) is specified, which is four-wavelength division multiplexing (WDM) with the bit rate of 25 Gb/s with non-return-to-zero (4λ x 25-Gb/s NRZ). To upgrade the total throughput for 400-Gb/s, three options have been mainly discussed, which are to increase the number of wavelengths (horizontal axis in the figure), to increase the bit rate per wavelength (vertical axis), or to use a higher-order modulation (HOM) format. In the early stage of the discussion, 16λ x 25-Gb/s NRZ was the promising candidate for 400GbE from the perspective of technical similarity to 100GbE [4], [5]. In the latest discussion, the focus has shifted to how to reduce the number of wavelengths by increasing the bit rate of each wavelength and applying HOM. For 400-Gb/s throughput by 8λ, the reports and contributions present bit rate per wavelength of 50-Gb/s not only with NRZ [6], [7] but also with four-level pulse amplitude modulation (PAM4) [8], [9]. For 4λ WDM, 100-Gb/s PAM4 [10], [11], discrete multi-tone (DMT) [12], [13], and carrier-less amplitude phase modulation (CAP) [14] have been proposed. To date, the plan regarding 400GbE is to adopt 8λ x 50-Gb/s PAM4 for 2-km and 10-km reach. However, studies of HOM with WDM will exploit future technology for flexible network flexibility by such as FlexEthernet [15], and future 1-Tb/s link.

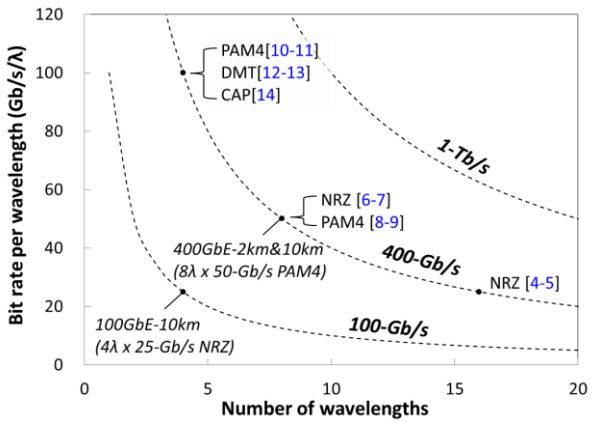

Fig. 1 Recent research trends in 100GbE-and-beyond datacom.

In this paper, we report several integrated devices and applications for 100GbE-and-beyond datacom. In the next section, we first review the basic configuration of Ethernet transceivers regarding several form-factors. Then, we explain integration technology for a 100GbE optical sub-assembly, for which we demonstrate a low-loss optical demultiplexer, low-loss optical coupling, and satisfactory operation for 10-km reach. In the following section, we describe our recent studies on 400-Gb/s aggregation with 16λx 25-Gb/s NRZ and 8λ x 50-Gb/s PAM4 using the 100GbE optical sub-assemblies together with cyclic arrayed waveguide gratings (AWGs).

2. Ethernet Transceivers

Figure 2 shows the basic configuration of a 100GbE

Manuscript received June 12, 2015.
Manuscript revised October 5, 2015.

[†]The authors are with NTT Device Innovation Center, NTT Corporation, Atsugi-shi, 243–0198 Japan.
[††]The authors are with NTT Device Technology Laboratories, NTT Corporation, Atsugi-shi, 243–0198 Japan.
a) E-mail: doi-yoshiyuki@ntt-el.com

DOI: 10.1587/transele.E99.C.157

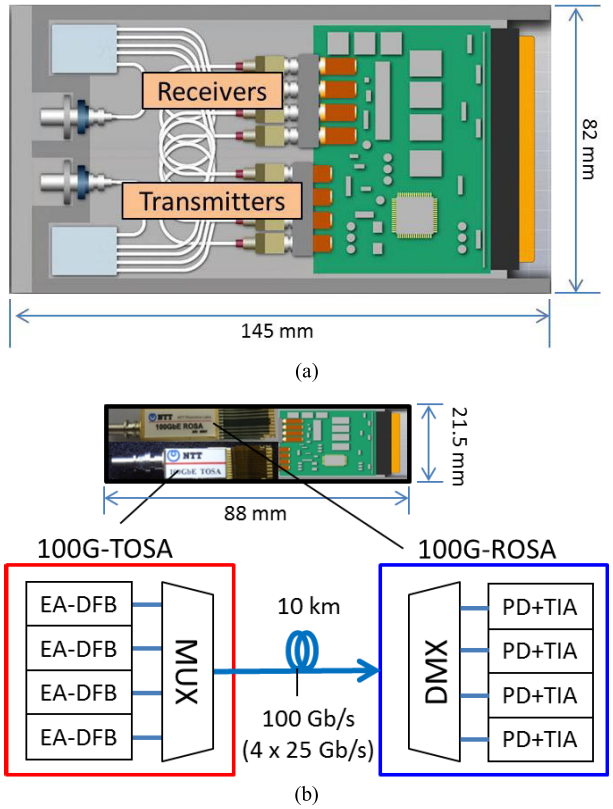

Fig. 2 Configurations of Ethernet transceivers. (a) 100GbE CFP transceiver. (b) CFP4 transceiver and its circuit diagram.

transceiver. Since the dawn of 100GbE, a C form-factor pluggable (CFP) transceiver [16], as shown in Fig. 2 (a), has been used. This is specified in an MSA, and the transceiver is 82 x 145 x 13.6 mm^3 in size. However, as datacom networks require not only higher data rates but also compact transceivers that can be mounted in a limited space, CFP is being replaced with the more compact form-factor of CFP2 and CFP4.

Figure 2 (b) shows the size of CFP4 and its circuit diagram. CFP4, which is 21.5 × 89 × 9.5 mm^3 in size, can extend total capacity in a line card to 3.2 Tb/s, which is eight times denser than the 400 Gb/s of CPF. The CFP in Fig. 2 (a) consists of many discrete devices for transmitters and receivers, such as laser diodes, photodiodes (PDs), and optical filters. Although the performance of each device can be ensured by testing individually, the large footprint is inevitable. For compactness, a key feature of CFP4 is the integration of these optical and electrical devices. In contrast to the many parts in CFP, compact modules of a 100GbE transmitter optical sub-assembly (100G-TOSA) and receiver optical sub-assembly (100G-ROSA) are installed in CFP4. The TOSA integrates four-channel (4-ch) light sources, such as distributed-feedback lasers integrated with electroabsorption modulators (EA-DFBs) and an optical multiplexer (MUX). The ROSA consists of four-channel PDs, trans-impedance amplifiers (TIAs), and a demultiplexer (DMX).

Various integration technologies have been reported for the optical sub-assembly. For the 100G-TOSA, monolithic integration is reported in [17], [18]. In these cases, a 4-ch laser array with four wavelength lanes and a 4 x 1 multimode interferometer (MMI) optical coupler are integrated in a single chip. Although the monolithic integration provides excellent compactness, the yield degradation of the laser array must be managed. The TOSAs reported in [19]–[21] are constructed by using free-space optics to optimize optical coupling, but there are yet many optical components such as lenses and wavelength filters.

We have newly developed an AWG filter for our 100G-ROSA. The 10-km 100GbE uses 4-λ WDM with the spacing of 4.5 nm or 800 GHz, which is called LAN-WDM. With regards to the optical WDM filters, thin-film filters (TFFs) [22], [23] have been used in coarse WDM (CWDM) systems, which have a wider passband of 20 nm, However, an optical sub-assembly that uses TFFs for 100GbE, such as ones reported in [24], [25], requires a narrower filter passband for LAN-WDM and more precise assembly accuracy than that for CWDM. In addition, future systems such as 400GbE and terabit Ethernet are supposed to use more wavelengths such as 8 or 16. Therefore, WDM filters based on planar lightwave circuits (PLCs), such as AWGs, are very promising for meeting such fabrication and future scalability requirements in datacom.

3. Optical Sub-Assembly for 100G Ethernet

In this section, we review our integration technology for optical sub-assemblies for 100GbE. Here we focus on a receiver, a 100G-ROSA, which can be applied to 10-km reach and a CFP4 transceiver package [26]. This ROSA employs a low-loss silica-based AWG demultiplexer, a 4-ch PD and a 4-ch TIA. In this work, we used p-i-n PDs and limiting TIAs for the 100G-ROSA. However, the ROSA can use APDs for a much larger sensitivity margin for longer transmission reach [27], and the limiting TIAs can be replaced with linear ones to improve the waveform distortion for amplified HOM signals such as those with PAM and DMT formats.

3.1 100G-ROSA Configuration

Figure 3 (a) shows a photograph of the 100G-ROSA. It consists of a hermetically sealed metal package, a receptacle for the LC connector, a first lens, and flexible printed circuits (FPCs). In the package, a PLC sub-block including an AWG and PD is assembled together with a four-channel TIA. The size of the package is W7 x L20 x H6 mm^3 excluding the LC receptacle and FPCs, which makes it small enough to be stored in CFP4 form factors.

The PLC sub-block shown in Fig. 3 (b) is the key structure for low-loss, high-stability optical coupling. It comprises a DMX-AWG, a second collimating lens, an output lens array, and a PD array. The four-channel InGaAs/InP-based PD chip is flip-chip mounted on a ceramic carrier and attached to the output lens via spacers. A

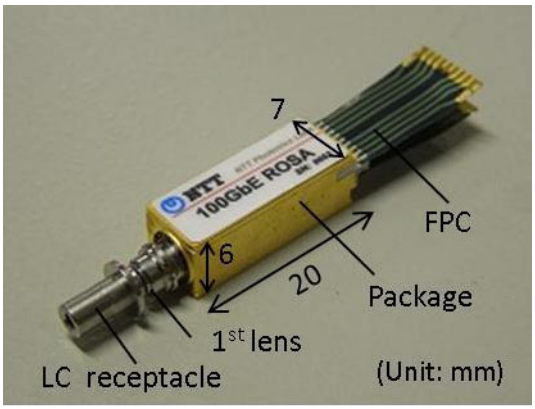

(a)

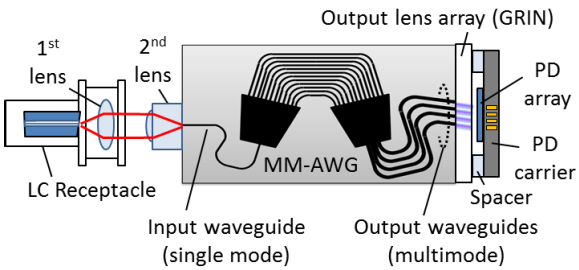

(b)

Fig. 3 ROSA configuration. (a) Photograph. (b) PLC sub-block.

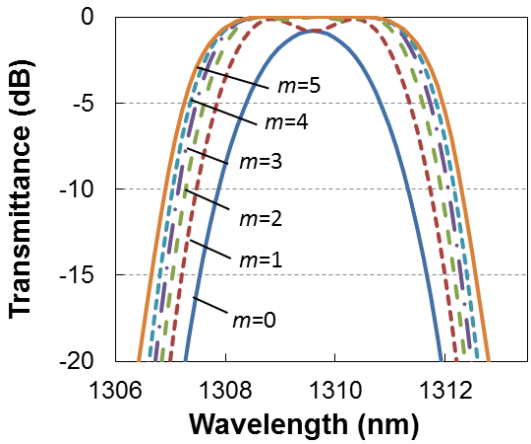

(a)

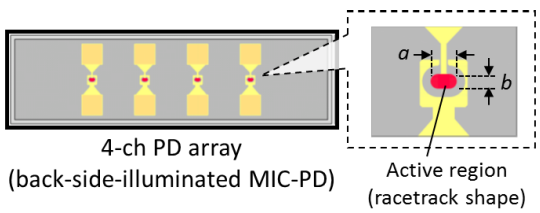

(b)

Fig. 4 Design of MM-AWG and optical coupling. (a) Calculation of spectral shape of MM-AWG. The parameter m is the mode number taken into account. (b) Racetrack shape in 4-ch PD array.

second input lens is directly attached to the PLC. A graded-index (GRIN) micro-lens array is also fixed directly to the edge of the output waveguides. By integrating these parts as one sub-block, this configuration enables high stability in optical coupling and responsivity of the ROSA against environmental conditions. The coupling structure between the PLC and PDs is based on the integrated receiver reported previously [28]. The main difference from the reported one is the use of a flat-top AWG with multimode output waveguides (MM-AWG) with optimized optical coupling between it and lens-coupled PDs, as described in the next section.

3.2 Low-Loss AWG and Low-Loss Optical Coupling

Compared with the conventional AWG with single-mode output waveguides, the MM-AWG with multimode waveguides provides a widened passband with low loss [29]. We have already developed integrated receivers for CWDM using MM-AWGs with $\Delta = 0.75\%$ for 10-Gb/s throughput (8λ x 1.25-Gb/s NRZ) [30] and 1.5% for 40-Gb/s throughput (4λ x 10-Gb/s NRZ) [31]. Here we applied the AWG for narrower channel spacing in LAN-WDM, as well as for higher Δ of 2% to reduce the chip size. Figure 4 (a) shows the dependence of the spectral shapes of the MM-AWG on the number of modes. As the width of the output waveguides is increased, a higher number of modes are generated. As shown in the figure, the more modes are multiplexed, the more the spectral shape becomes flattened.

Even if the spectral shape is flat in the MM-AWG itself, poor coupling with PDs causes degradation of received spectral shape. To detect all of the multimode beams efficiently, a racetrack shape is used in the active area of PDs, as schematically shown in Fig. 4 (b). The shape was optimized in terms of the ratio of waveguide width and height, a/b. The appropriate ratio was around 2 in our design. The PDs have other features to obtain high responsivity by using a configuration with both back-side illumination and a maximized induced current (MIC) structure [32]. The responsivity and 3-dB-down bandwidth of the PDs are 0.95 A/W and 23 GHz in the 1300-nm LAN-WDM band, respectively.

3.3 Receiver Performance

Figure 5 (a) shows the responsivity spectrum of our fabricated ROSA at room temperature. A flat-top spectrum was observed, and the maximum responsivity reached as high as 0.7 A/W for all lanes. The isolation between adjacent lanes is more than 25 dB in the 368-GHz passband, which is indicated between the vertical dashed lines in the figure. The breakdown of the optical loss is as follows: AWG loss of 0.8 dB, PLC-to-PD coupling loss of 0.3 dB, PLC-to-receptacle loss of 0.3 dB. The 0.5-dB bandwidth was over 500 GHz as expected, and, as a result, there was no temperature control or athermalization for the AWG of the 100G-ROSA. We further performed several environmental tests, such as temperature tracking from -5 to 80°C, high-temperature storage at 85°C, and mechanical shock. The loss change was suppressed to less than 0.2 dB, which reveals the high

stability of our assembly owing to the use of the PLC sub-block structure.

We measured the bit-error-rate (BER) characteristics of the fabricated ROSA in 100-Gb/s (4 × 25 Gb/s) operation. As shown by the solid lines in Fig. 5 (b), we measured the BERs in a single-channel back-to-back (B-to-B) operation. Here we used a $LiNbO_3$ Mach-Zehnder (LN) modulator as the source of an ideal optical signal. The input signal was a 25.78-Gb/s NRZ $2^{31} - 1$ pseudo-random bit sequence (PRBS), and the extinction ratio (ER) ranged from 10.4 to 10.8 dB. The figure shows that a minimum receiver sensitivity of less than −13.4 dBm was successfully achieved at a BER = 10^{-12}. Since the standard receiver sensitivity is an optical modulation amplitude (OMA) of −8.6 dBm in 100GBASE-LR4, the margin is more than 4.8 dB. Then, to confirm the penalties caused by crosstalk from adjacent and non-adjacent lanes, we measured the BERs during multi-channel operation. They are shown as the broken lines in the figure. The BERs for lanes 0, 1, and 2 were measured while the transmitter optical power of lane 3 was intentionally set 5 dB higher than that of lanes 0-2 as an aggressor. The penalty was as low as 0.4 dB from the adjacent lane, 0.1 dB from the second adjacent lane, and negligible from the third adjacent lane. These results clearly show our fabricated ROSA has sufficient quality and an appropriate size to be applied to compact 100GbE transceivers such as CFP2 or CFP4. This assembly technology would be applicable for compact integrated receivers not only for 100GbE but also for beyond-400-Gb/s systems.

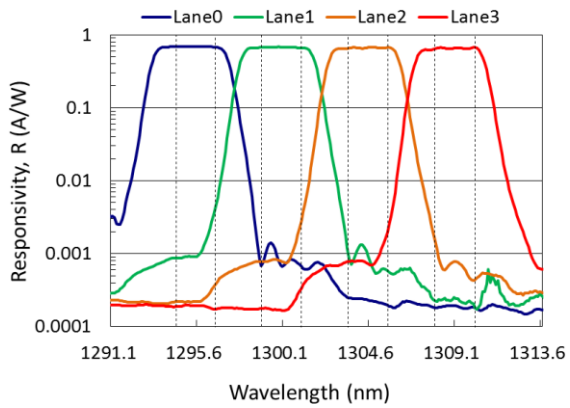

(a)

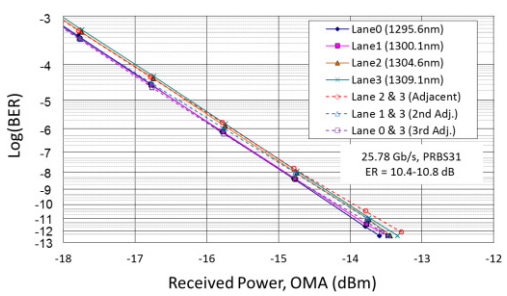

(b)

Fig. 5 Experimental results for the ROSA. (a) Responsivity spectrum. (b) BER of single-channel and multi-channel B-to-B operations with LN modulator.

4. Studies of 400-Gb/s Aggregation

For early aggregation of higher bit rates without massive capital expenditure upon replacement, it is important to build networks by extending current technology as efficiently as possible. In line with such a requirement, we have studied simple WDM 400-Gb/s links that utilize newly designed cyclic AWGs and current 100GbE TOSA/ROSAs. The key feature for multiplexing is the use of a cyclic AWG with the frequency spectrum range (FSR) of 800 GHz, which is the same as of the frequency spacing of LAN-WDM.

4.1 400G by 16λ x 25-Gb/s NRZ

Our first proposal is the 400-Gb/s WDM configuration shown in Fig. 6 (a) [5]. It consists of four 4λ x 25-Gb/s 100G-TOSAs, four 100G-ROSAs, and cyclic AWGs. Each TOSA transmits 4 x 25-Gb/s NRZ signals with a slightly shifted wavelength with 100-GHz spacing from an adjacent TOSA wavelength, and then four wavelength groups generated by the four TOSAs are multiplexed through the MUX into WDM signal of 400 Gb/s (16λ x 25 Gb/s NRZ). Transmitted WDM signal is divided into four wavelength groups in the DMX-AWG, which are respectively fed to the four ROSAs. The ROSAs can detect any wavelength group of the transmitted signal because the groups are allocated within the LAN-WDM passband, 368 GHz, which can be

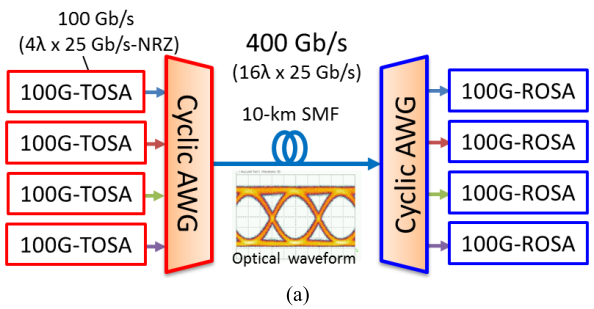

(a)

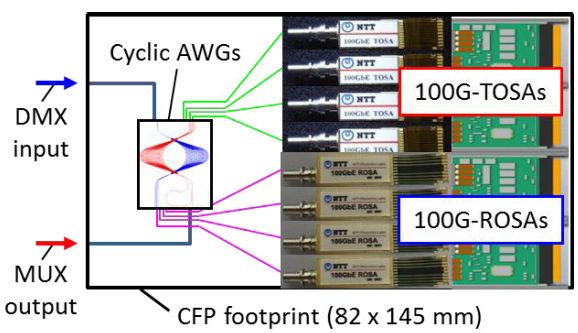

(b)

Fig. 6 Schematic configuration of (a) proposed WDM with 16λ x 25-Gb/s NRZ and (b) 400G transceiver within CFP footprint.

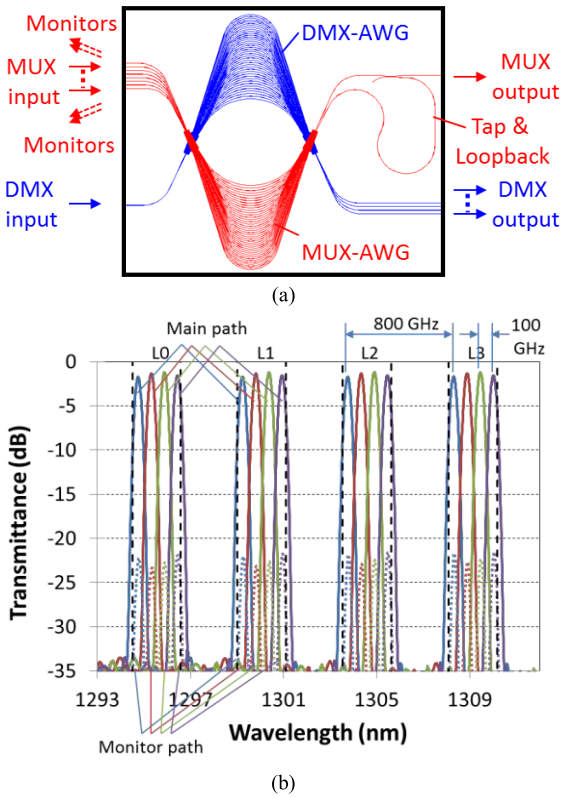

Fig. 7 Cyclic AWG. (a) Circuit design. (b) Measured transmittance in main paths and monitor paths of MUX-AWG.

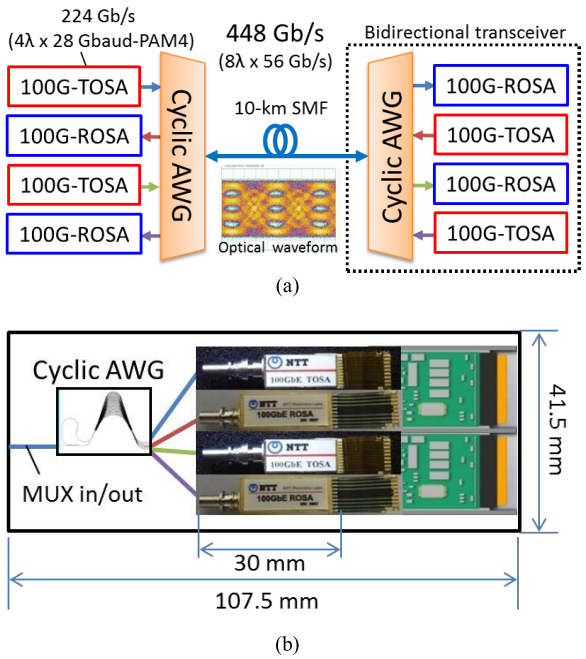

Fig. 8 Schematic configuration of (a) proposed bidirectional WDM with 8λ x 50-Gb/s PAM4 and (b) 400G bidirectional transceiver within CFP2 footprint.

demultiplexed by a LAN-WDM filter. Figure 6 (b) shows a schematic image of the 400G transceiver. Since our compact 100G-TOSAs and ROSAs are applied together with the integrated cyclic AWGs, the footprint of the transceiver is within the 82 x 145 mm^2 of the CFP transceiver.

The circuit design of the cyclic AWGs is shown in Fig. 7 (a). The silica-based AWGs have the refractive index difference of 1.5% and are 20 x 15 mm^2 in size. With connections of single-mode fibers, the insertion loss of a single AWG is around 1 dB. The circuit also has functionality for wavelength control by adding four monitor ports at the MUX input side and a loopback circuit at the MUX output side. The summation of the optical powers of the four lanes detected from a monitor port is fed back to the temperature and driving-current control of the TOSA. Figure 7 (b) is the measured spectrum of the MUX-AWG, which shows the 800-GHz cyclic nature of the AWG for the main and monitor paths within the passband of LAN-WDM. In the experimental results for 10-km transmission over the WDM link with our 100G-TOSAs [21] and ROSAs, we obtained minimum receiver sensitivity at the BER of 10^{-12} of better than −10.5 dBm for all lanes with single-channel operation of 25-Gb/s NRZ. There is a 3-dB sensitivity penalty due to the smaller operating bandwidth of the TOSA and waveform filtering by the cyclic AWGs. However, there are still sufficient margins of 1.9 and 3.7 dB against the −8.6 dBm in ideal signals and −6.8 dBm in stressed signals specified in the criteria of 100GbE, respectively.

4.2 Bidirectional 400G by 8λ x 50-Gb/s PAM4

Our other proposed 400-Gb/s configuration is a bidirectional link [9] that uses 8λ x 50-Gb/s PAM4 The 400GbE standard, which covers transmission reach of up to 10 km, will wire an optical fiber cable for each direction, or, in other words, allow duplex transmission. However, for future installations of large numbers of fibers in networks, cost-effective and simplified system development will be preferable by adopting bidirectional transceivers, which are widely used in metropolitan-area networks and passive optical networks.

The proposed bidirectional configuration is shown in Fig. 8 (a). It also utilizes 100GbE optical sub-assemblies and cyclic AWGs for the MUX and DMX. To ramp up the total bit rate to 400 Gb/s with only eight wavelengths in each direction, PAM4 is applied for each lane. The output of each 100G-TOSA with the bit rate of 224 Gb/s has four channels of 28-Gbaud PAM4 signal with the frequency spacing of 800 GHz. The 400-Gb/s (448 Gb/s, including excess bits for error correction) WDM of 8λ x 50-Gb/s PAM4 is obtained by connecting the outputs of the two 100G-TOSAs to the cyclic AWG. The optical waveform of 28-Gbaud PAM4 signal with clearly opened eyes is shown in the inset of the figure. The proposed configuration not only achieves bidirectional transmission with 8λ-WDM but also provides a compact form-factor in Ethernet transceivers as schematically shown in Fig. 8 (b). Since the number of optical components is reduced by adopting a higher-order PAM4 format together with compact 100G-TOSAs and ROSAs, the footprint of the transceiver is within the 107.5 x 41.5 mm^2 of the CFP2 transceiver.

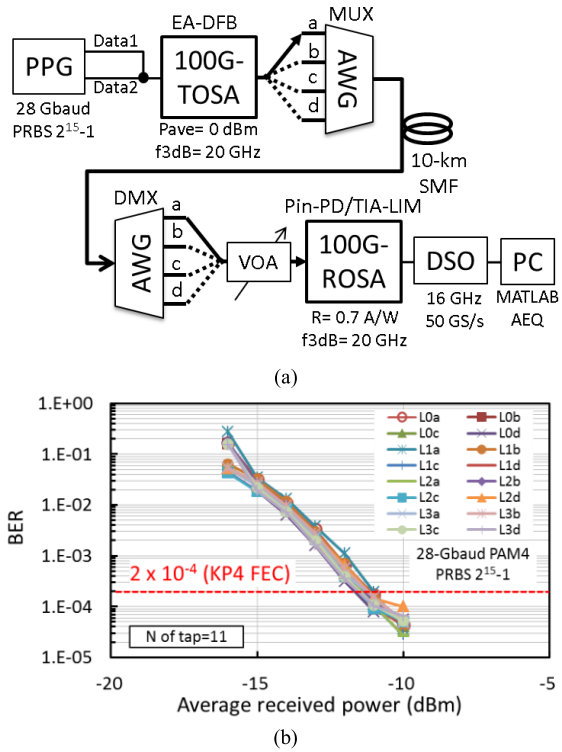

Fig. 9 Test results. (a) Experimental setup. (b) BER for 16 wavelengths.

We confirmed the feasibility of the WDM link in 10-km transmission with the setup shown in Fig. 9 (a). The PAM4 signal with the amplitude of 1.2 Vpp was created by the summation of two binary signals of a 28-Gb/s PRBS with the length of $2^{15} - 1$. For single-channel operation in the 100G-TOSA, the wavelength of each channel was chosen and connected to the proper input of the AWG. The received signal was demodulated with an adaptive equalizer in offline digital signal processing. At the BER of 2×10^{-4}, assuming RS (544, 514) FEC defined in 100GBASE-KP4 (IEEE 802.3bj), we observed the minimum receiver sensitivity of better than −11 dBm for all channels as shown in Fig. 9 (b). We also confirmed that, thanks to sufficient suppression of optical crosstalk in the cyclic AWGs, there was negligible degradation of the BER even when an adjacent lane in the forward or reverse direction was added.

5. Conclusions

Recent trends in photonic integration technologies for 100GbE-and-beyond datacom were reviewed. Wavelength scalability, higher bit rates, and more sophisticated modulation will be exploited for 400GbE and future functional WDM links. For a compact form-factor of Ethernet transceivers, an integrated optical sub-assembly for 100GbE with 4λ x 25-Gb/s NRZ was reported. To ramp up the bit rate to 400-Gb/s throughput with higher wavelength scalability, 16λ x 25-Gb/s NRZ and 8λ x 50-Gb/s PAM4 were demonstrated by utilizing 100GbE devices and functional cyclic AWGs. With the growing demands on datacenter and mobile networks, photonic integration will play a more important role for datacom.

Acknowledgments

We thank Y. Nasu, I. Ogawa and E. Yoshida for their cooperation in this work. We also thank K. Murata, A. Kaneko and S. Suzuki for their continuous support.

References

[1] D. Law, "IEEE 802.3 Industry Connections Ethernet Bandwidth Assessment," IEEE 802.3 BWA Ad Hoc Report, July 2012.
[2] "IEEE Standard 802.3ba-2010, 40 Gb/s and 100 Gb/s Ethernet." [Online]. Available: http://www.ieee802.org/3/ba/
[3] "IEEE P802.3bs 400 Gb/s Ethernet Task Force." [Online]. Available: http://www.ieee802.org/3/bs/
[4] R. Gutierrez-Castrejon and P. Torres-Ferrera, "Design and Technical Feasibility of Next 400 GbE 40-km PMD Based on 16 x 25 Gbps Architecture," J. Lightw. Technol., vol.31, no.14, pp.2386–2393, July 2013.
[5] Y. Doi et al., "400GbE Demonstration Utilizing 100GbE Optical Sub-Assemblies and Cyclic Arrayed Waveguide Gratings," Proc. Optical Fiber Communication Conference, Paper M2E.2, San Francisco, CA, USA, March 2014.
[6] M. Shirao and K. Kojima, "Proposal of 8 x 50G NRZ Specification for 400GbE 2km PMD," IEEE 802.3 400 Gb/s Ethernet Task Force, Plenary Meeting, San Antonio, TX, USA, Nov. 2014.
[7] S. Kanazawa, T. Fujisawa, H. Ishii, K. Takahata, Y. Ueda, R. Iga, and H. Sanjoh, "High-speed (400 Gb/s) Eight-channel EADFB Laser Array Module Using Flip-chip Interconnection Technique," IEEE J. Sel. Topics Quantum Electron., vol.21, no.6, p.1501106, 2015.
[8] C. Cole, "400Gb/s 2km & 10km duplex SMF PAM-4 PMD Baseline Specifications," IEEE 802.3 400 Gb/s Ethernet Task Force, Interim Meeting, Pittsburgh, PA, USA, May 2015.
[9] Y. Doi, T. Ohyama, Y. Nakanishi, T. Yoshimatsu, S. Soma, H. Yamazaki, and M. Oguma, "Bidirectional 400-Gb/s transmission by 100GbE Optical Sub-Assemblies and a Cyclic Arrayed Waveguide Grating," Proc. Optical Fiber Communication Conference, Paper Th1G.5., Los Angeles, CA, USA, March 2015.
[10] R. Hirai and N. Kikuchi, "Experimental Demonstration of 100G/lambda Nyquist-PAM4 Transmission with Digital Pre-Equalization of Chromatic Dispersion for Extended-Reach 400GbE," in Proc. Optical Fiber Communication Conference, vol.2015, Paper Th4A.6, Los Angeles, CA, USA, March 2015.
[11] T. Chan and W.I. Way, "112 Gb/s PAM4 Transmission Over 40km SSMF Using 1.3 μm Gain-Clamped Semiconductor Optical Amplifier," in Proc. Optical Fiber Communication Conference, Paper Th3A.4., Los Angeles, CA, USA, March 2015.
[12] T. Tanaka, M. Nishihara, T. Takahara, W. Yan, L. Li, Z. Tao, M. Matsuda, K. Takabayashi, and J. Rasmussen, "Experimental Demonstration of 448-Gbps+ DMT Transmission over 30-km SMF," in Proc. Optical Fiber Communication Conference, Paper M2I.5, San Francisco, CA, USA, March 2014.
[13] H. Isono, H. Sakamoto, Y. Miyaki, T. Tanaka, T. Takahara, and B. Martin, "Discrete Multi-Tone for 400GbE 10km reach," IEEE802.3 Norfork Interim Meet., 2014.
[14] M.I. Olmedo, T. Zuo, J.B. Jensen, Q. Zhong, X. Xu, and I.T. Monroy, "Towards 400GBASE 4-lane Solution Using Direct Detection of MultiCAP Signal in 14 GHz Bandwidth per Lane," Proc. Optical Fiber Communication Conference, Paper PDP5C.10., Anaheim, CA, USA, March 2013.
[15] "FlexEthernet Project Start Proposal," contributed to assist the Optical Internetworking Forum (OIF), oif2015.039.02, 2015.
[16] "CFP Multi-Source Agreement." [Online]. Available: http://www.

cfp-msa.org/
[17] S. Kanazawa, T. Fujisawa, N. Nunoya, A. Ohki, K. Takahata, H. Sanjoh, R. Iga, and H. Ishii, "Ultra-Compact 100 GbE Transmitter Optical Sub-Assembly for 40-km SMF Transmission," J. Lightw Technol., vol.31, no.4, pp.602–608, Feb. 2013.
[18] W. Kobayashi, S. Kanazawa, Y. Ueda, T. Ohno, T. Yoshimatsu, T. Shindo, H. Sanjoh, H. Ishii, S. Matsuo, and M. Itoh, "Monolithically Integrated Directly Modulated DFB Laser Array with MMI Coupler for 100GBASE-LR4 Application," in Proc. Optical Fiber Communication Conference, Paper Tu3I.2, Los Angeles, CA, USA, March 2015.
[19] T. Saeki, S. Sato, M. Kurokawa, A. Moto, M. Suzuki, K. Tanaka, K. Tanaka, N. Ikama, and Y. Fujimura, "100Gbit/s Compact Transmitter Module Integrated with Optical Multiplexer," in Proc. Photonics Conference, TuG3.2., 2013.
[20] T. Murao, N. Yasui, T. Shinada, Y. Imai, K. Nakamura, M. Shimono, H. Kodera, Y. Morita, A. Uchiyama, H. Koyanagi, and H. Aruga, "Integrated Spatial Optical System for Compact 28-Gb/s × 4-lane Transmitter Optical Subassemblies," IEEE Photon. Technol. Lett., vol.26, no.22, pp.2275–2278, Nov. 2014.
[21] T. Ohyama, A. Ohki, K. Takahata, T. Ito, N. Nunoya, H. Mawatari, T. Fujisawa, S. Kanazawa, R. Iga, and H. Sanjoh, "Transmitter Optical Subassembly Using a Polarization Beam Combiner for 100Gbit/s Ethernet over 40 km Transmission," J. Lightw Technol., vol.33, no.10, pp.1985–1992, May 2015.
[22] G.E. Tangdiongga, T.G. Lim, J. Li, C.W. Tan, P.V. Ramana, Y.Y. Chai, S. Maruo, and J.H.-S. Lau, "Optical Design of 4-channel TOSA/ROSA for CWDM Applications," Proc. SPIE, 2008, vol.6899, no.2008, p.68990I.
[23] L. Ralf, "WDM Filters for CWDM," in Coarse Wavelength Division Multiplexing: Technologies and Applications, CRC Press, 2007.
[24] H. Aruga, K. Mochizuki, H. Itamoto, R. Takemura, K. Yamagishi, M. Nakaji, and A. Sugitatsu, "Four-channel 25Gbps Optical Receiver for 100Gbps Ethernet with Built-in Demultiplexer Optics," Proc. European Conference and Exhibition on Optical Communication, pp.1623–1625, Paper Th.10.D.4., 2010.
[25] J.K. Lee, J.Y. Huh, S.-K. Kang, and Y.-S. Jang, "Analysis of Dimensional Tolerance for an Optical Demultiplexer of a Highly Alignment Tolerant 4 × 25 Gb/s ROSA Module," Opt. Express, vol.22, no.4, pp.4307–4315, Feb. 2014.
[26] Y. Doi, M. Oguma, M. Ito, I. Ogawa, T. Yoshimatsu, T. Ohno, E. Yoshida, and H. Takahashi, "Compact ROSA for 100-Gb/s (4 x 25 Gb/s) Ethernet with a PLC-based AWG demultiplexer," Proc. Optical Fiber Communication Conference/National Fiber Optic Engineers Conference, Paper NW1J.5., Anaheim, CA, USA, March 2013.
[27] T. Yoshimatsu, M. Nada, M. Oguma, H. Yokoyama, T. Ohno, Y. Doi, I. Ogawa, and E. Yoshida, "Compact and high-sensitivity 100-Gb/s (4 x 25 Gb/s) APD-ROSA with a LAN-WDM PLC demultiplexer," Proc. European Conference on Optical Communication, Paper Th.3.B.5., 2012.
[28] S. Tsunashima, F. Nakajima, Y. Nasu, R. Kasahara, T. Saida, T. Yamada, K. Sano, T. Hashimoto, H. Fukuyama, H. Nosaka, and K. Murata, "Silica-based, Compact and Variable-optical-attenuator Integrated Coherent Receiver with Stable Optoelectronic Coupling System," Opt. Express, vol.20, no.24, pp.1749–1750, 2012.
[29] M.R.R. Amersfoort, C.R. de Boer, F.P.G.M. van Ham, M.K.K. Smit, P. Demeester, J.J.G.M. van der Tol, and A. Kuntze, "Phased-array Wavelength Demultiplexer with Flattened Wavelength Response," Electron. Lett., vol.30, no.4, pp.300–302, Feb. 1994.
[30] Y. Doi, M. Ishii, S. Kamei, I. Ogawa, S. Mino, T. Shibata, Y. Hida, T. Kitagawa, and K. Kato, "Flat and High Responsivity CWDM Photoreceiver using Silica-based AWG with Multimode Output Waveguides," Electron. Lett., vol.39, no.22, pp.1603–1604, 2003.
[31] Y. Doi, T. Ohyama, T. Hashimoto, S. Kamei, A. Ohki, M. Ishii, M. Yanagisawa, and S. Mino, "A Coarse-WDM Transmitter/Receiver for 10 Gb/s× 4ch Interconnection using a Silica-based Planar Lightwave Circuit," Proc. Conference on Lasers and Electro-Optics, Paper. CTuW1., 2004.
[32] Y. Muramoto and T. Ishibashi, "InP/InGaAs pin Photodiode Structure Maximising Bandwidth and Efficiency," Electron. Lett., vol.39, no.24, pp.1749–1750, 2003.

Yoshiyuki Doi received the M.S. degrees in physics and Ph.D. in material science from Shinshu University, Japan in 1997 and 2007, respectively. Since 1997, he has been engaged in research at the Nippon Telegraph and Telephone Corporation (NTT) on integrated photonics devices for telecom, datacom, and microwave photonics, such as high-speed receivers, large-scale optical switches and high-functional optical modulators. He is now a Senior Research Engineer at the NTT Device Innovation Center, Kanagawa, Japan.

Takaharu Ohyama received the B.E. degree from Kyushu Institute of Technology, Japan in 1992 and the M.E. degree from Kyushu University, Japan, in 1994. Since joining NTT Opto-electronics (Photonics) Laboratories, NTT Corporation, Japan, he has been engaged in research on optical integration module. He is currently with the NTT Device Innovation Center, Kanagawa, Japan.

Toshihide Yoshimatsu received the B.E. and M.E. degrees in applied physics from Tohoku University, Miyagi, Japan, in 1998 and 2000, respectively. He joined NTT Photonics Laboratories, NTT Corporation in Kanagawa, Japan, in 2000. He has been engaged in research and development of ultrafast opto-electronic devices. He is currently a Senior Research Engineer with the NTT Device Innovation Center, Kanagawa, Japan.

Tetsuichiro Ohno was born in Osaka, Japan in 1966. He received the B.E. degree in 1989, the M.E. degree in 1991, both from Osaka University, and the Ph.D. degree in 1999 from Shizuoka University, Japan. In 1991, he joined NTT Opto-electronics Laboratories, and has been engaged in research on opto-electronics devices. He is now a Senior Research Engineer with the NTT Device Innovation Center, Kanagawa, Japan.

Yasuhiko Nakanishi received the M.S. degree in engineering from Hokkaido University, Japan, in 2002. He has been engaged in research and development of optical communications systems and devices. He is now a Senior Research Engineer at the NTT Device Innovation Center, Kanagawa, Japan.

Shunichi Soma received the M.S. degree in electronic engineering from Tohoku University in 1999. In 1997, he joined NTT Photonics Laboratories, and has been working on silica-based planar lightwave circuit (PLC) devices and integrated photonics. He is now a Senior Research Engineer at NTT Device Innovation Center, Kanagawa, Japan.

Hiroshi Yamazaki received the M.S. degree in human and environmental studies from Kyoto University, Kyoto, Japan, in 2005, and the Dr. Eng. degree in electronics and applied physics from Tokyo Institute of Technology, Tokyo, Japan, in 2015. In 2005, he joined NTT Photonics Laboratories, Kanagawa, Japan, where he has been engaged in research on optical waveguide devices for fiber transmission systems using advanced modulation formats. He is currently with NTT Device Technology Laboratories, Kanagawa, Japan.

Manabu Oguma received the B.S. and M.S. degrees in applied physics from Tohoku University, Miyagi, Japan, in 1989 and 1991, respectively. He joined the NTT Opto-Electronics Laboratories, Ibaraki (now Device Technology Laboratories, Atsugi), Japan, in 1991, where he has been engaged in research on silica-based planar light wave circuits (PLC). He is currently with NTT Device Technology Laboratories, Kanagawa, Japan.

Toshikazu Hashimoto received the B.S. and M.S. degrees in physics from Hokkaido University, Japan, in 1991 and 1993, respectively. Since joining NTT Laboratories in 1993, he has been engaged in research on hybrid integration of semiconductor lasers and photodiodes on silica-based planar lightwave circuits and in theoretical research on the wavefront matching method. He is currently with NTT Device Technology Laboratories, Kanagawa, Japan.

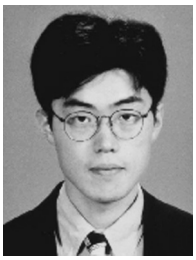

Hiroaki Sanjoh was born in Hokkaido, Japan in 1968. He received the B.E. and M.E. degrees in applied physics from Hokkaido University, Sapporo, Japan, in 1990 and 1992, respectively. In 1992, he joined Nippon Telegraph and Telephone (NTT) Optoelectronics Laboratories, Kanagawa, Japan. He is currently with the NTT Device Innovation Center, Kanagawa, Japan, where he is engaged in developmental research on optical sub-assembly modules.